Table II. Fractional Coordinates[a] and Isotropic Thermal Parameters[b] for $Y_2(OSiPh_3)_6$

	x	y	z	$10B_{iso}$, Å^2
Y(1)	478 (1)	4582 (1)	9324.4 (3)	18
Si(2)	-683 (2)	3330 (2)	10480 (1)	20
Si(3)	-1174 (2)	4509 (2)	8040 (1)	24
Si(4)	2269 (2)	2949 (2)	9096 (1)	26
O(5)	-323 (3)	4186 (3)	10114 (2)	19
O(6)	-469 (4)	4544 (4)	8613 (2)	26
O(7)	1504 (4)	3640 (4)	9320 (2)	26
C(8)	-1280 (5)	2533 (5)	9975 (4)	23
C(9)	320 (5)	2792 (6)	10876 (3)	23
C(10)	-1521 (5)	3800 (5)	11030 (4)	23
C(11)	-2432 (5)	4439 (5)	8299 (4)	24
C(12)	-1027 (6)	5478 (6)	7545 (4)	29
C(13)	-924 (5)	3511 (6)	7588 (4)	26
C(14)	2505 (6)	3165 (5)	8287 (4)	26
C(15)	1815 (6)	1807 (6)	9173 (4)	32
C(16)	3366 (6)	3038 (6)	9561 (4)	28
C(17)	224 (6)	1976 (6)	11138 (4)	27
C(18)	941 (7)	1559 (7)	11425 (5)	43
C(19)	1821 (8)	1946 (8)	11458 (5)	49
C(20)	1954 (6)	2738 (7)	11208 (4)	41
C(21)	1212 (6)	3173 (6)	10927 (4)	31
C(22)	-1388 (6)	3692 (6)	11649 (4)	34
C(23)	-2043 (8)	4033 (7)	12042 (4)	47
C(24)	-2820 (7)	4480 (7)	11828 (5)	44
C(25)	-2948 (6)	4611 (6)	11226 (4)	35
C(26)	-2295 (7)	4273 (6)	10835 (4)	32
C(27)	-759 (7)	2059 (7)	9589 (5)	48
C(28)	-1148 (9)	1441 (7)	9209 (4)	51
C(29)	-2072 (8)	1308 (7)	9195 (5)	52
C(30)	-2617 (8)	1760 (9)	9577 (8)	93
C(31)	-2213 (7)	2366 (8)	9967 (7)	69
C(32)	-2589 (6)	4249 (7)	8896 (4)	37
C(33)	-3512 (7)	4150 (8)	9093 (5)	49
C(34)	-4238 (7)	4239 (7)	8705 (5)	43
C(35)	-4099 (6)	4419 (7)	8109 (5)	41
C(36)	-3190 (6)	4519 (6)	7915 (4)	33
C(37)	-185 (7)	5572 (7)	7240 (4)	41
C(38)	-47 (7)	6282 (7)	6870 (5)	47
C(39)	-702 (8)	6924 (7)	6815 (5)	50
C(40)	-1516 (7)	6851 (7)	7112 (5)	46
C(41)	-1684 (7)	6136 (6)	7467 (4)	37
C(42)	-818 (7)	3517 (6)	6971 (4)	35
C(43)	-652 (6)	2750 (8)	6662 (4)	41
C(44)	-537 (7)	1979 (7)	6957 (5)	46
C(45)	-639 (8)	1951 (7)	7567 (5)	50
C(46)	-816 (7)	2709 (6)	7878 (4)	41
C(47)	1795 (6)	3320 (7)	7875 (4)	37
C(48)	1914 (6)	3479 (7)	7280 (4)	42
C(49)	2833 (7)	3467 (7)	7070 (4)	38
C(50)	3572 (6)	3316 (7)	7460 (4)	36
C(51)	3429 (6)	3163 (6)	8059 (4)	28
C(52)	1556 (7)	1293 (6)	8688 (5)	42
C(53)	1193 (9)	461 (8)	8774 (6)	67
C(54)	1116 (11)	141 (7)	9350 (7)	76
C(55)	1364 (10)	642 (7)	9824 (6)	63
C(56)	1711 (7)	1465 (6)	9749 (5)	42
C(57)	4046 (7)	2374 (7)	9562 (4)	39
C(58)	4870 (7)	2448 (9)	9907 (5)	54
C(59)	5068 (7)	3146 (9)	10249 (4)	53
C(60)	4411 (7)	3800 (7)	10264 (5)	45
C(61)	3586 (7)	3752 (6)	9925 (4)	34
C(62)	4144 (13)	9936 (11)	9655 (8)	90 (4)
C(63)	4164 (12)	10155 (11)	10266 (8)	95 (5)
C(64)	5015 (13)	9789 (11)	9409 (7)	95 (4)
C(65)	3502 (27)	9785 (25)	9286 (17)	119 (9)

[a] Fractional coordinates are $\times 10^4$. [b] Isotropic values for those atoms refined anisotropically are calculated by using the formula given by: Hamilton, W. C. *Acta Crystallogr.* **1959**, *12*, 609.

$Y_2(OSiMe_2{}^tBu)_6({}^tBuMe_2SiOH)$,[1] and $Y_2(OAr)_6(THF)_2$ (Ar = 2,6-$Me_2C_6H_3$),[6] which all have two bridging groups. The (paramagnetic) cerium(III) compound is rigorously centrosymmetric and adopts the diborane structure. It shows no bridge/terminal exchange by ^1H NMR spectroscopy at 25 °C. The yttrium siloxide compound (II) is rapidly fluxional (500-MHz ^1H NMR) among all sites. The aryloxide dimer containing THF has the structure of two square based pyramids sharing a basal edge. Two distinct aryl environments are detected in the proton NMR spectrum of the ring methyls. The provisional conclusion from these and related[4] data is that exchange of μ_2 and terminal OR groups is not extremely facile *except* when it is proton-catalyzed (e.g., $Y_2(OSiMe_2{}^tBu)_6({}^tBuMe_2SiOH)$). This relates to intramolecular exchange, but it also implies that dissociation of Y_2 species into monometal fragments is not rapid on the NMR time scale. Taken together with the variable metal coordination number observed in Y_2 species, this suggests that the "bridge-splitting" reactions of eq 1-4 occur by an associative mechanism.

Table III. Selected Bond Distances (Å) and Angles (deg) for $Y_2(OSiPh_3)_6$

Y(1)-O(5)	2.211 (5)	Si(3)-C(11)	1.903 (8)
Y(1)-O(5)′	2.288 (5)	Si(3)-C(12)	1.872 (9)
Y(1)-O(6)	2.058 (5)	Si(3)-C(13)	1.879 (9)
Y(1)-O(7)	2.062 (5)	Si(4)-O(7)	1.613 (6)
Si(2)-O(5)	1.642 (5)	Si(4)-C(14)	1.875 (9)
Si(2)-C(8)	1.859 (8)	Si(4)-C(15)	1.884 (9)
Si(2)-C(9)	1.856 (8)	Si(4)-C(16)	1.860 (9)
Si(2)-C(10)	1.879 (8)	Y(1)-Y(1)′	3.581 (1)
Si(3)-O(6)	1.607 (6)		
O(5)-Y(1)-O(5)′	74.54 (20)	Y(1)-O(5)-Y(1)′	105.46 (20)
O(5)-Y(1)-O(6)	112.03 (20)	Y(1)-O(5)-Si(2)	111.06 (25)
O(5)′-Y(1)-O(6)	105.42 (20)	Y(1)-O(5)′-Si(2)′	142.5 (3)
O(5)-Y(1)-O(7)	131.76 (20)	Y(1)-O(6)-Si(3)	177.8 (3)
O(5)′-Y(1)-O(7)	101.01 (20)	Y(1)-O(7)-Si(4)	162.3 (4)
O(6)-Y(1)-O(7)	115.29 (22)		

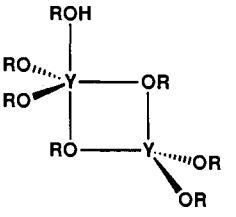

II (R = ^{t}BuMe$_2$Si)

Acknowledgment. This work was supported by the Department of Energy.

Supplementary Material Available: Tables of full crystallographic details and anisotropic thermal parameters (3 pages); a listing of observed and calculated structure factors (13 pages). Ordering information is given on any current masthead page.

Contribution from the Department of Chemistry, Michigan State University, East Lansing, Michigan 48824

Gold(I) vs Gold(III): Stabilization of Two Gold(I) Polyselenide Complexes, $[Au_2(Se_2)(Se_3)]^{2-}$ and $[Au_2(Se_2)(Se_4)]^{2-}$, by the Diselenide Unit

Song-Ping Huang and Mercouri G. Kanatzidis*

Received December 26, 1990

Introduction

The synthesis, structural characterization, and reactivity of heavier metal polychalcogenide (i.e. polyselenide and polytelluride) compounds are currently an active area of research[1,2] after intense

(5) Stecher, H. A.; Sen, A.; Rheingold, A. *Inorg. Chem.* **1989**, *28*, 3280.
(6) Evans, W. J.; Olofson, J. M.; Ziller, J. W. *Inorg. Chem.* **1989**, *28*, 4309.

(1) Kanatzidis, M. G. *Comments Inorg. Chem.* **1990**, *10*, 161-195.

0020-1669/91/1330-3572$02.50/0

Table I. Data for Crystal Structure Analyses of $(Ph_4P)_2[Au_2(Se_2)(Se_3)]$ (I), $[(Ph_3P)_2N]_2[Au_2(Se_2)(Se_3)]$ (II), and $(Ph_4P)_2[Au_2(Se_2)(Se_4)]$ (III)

	I	II	III
formula	$C_{48}H_{40}P_2Au_2Se_5$	$C_{72}H_{60}P_4N_2Au_2Se_5$	$C_{48}H_{40}P_2Au_2Se_6$
a, Å	10.381 (4)	12.166 (3)	28.409 (7)
b, Å	11.002 (5)	12.960 (5)	10.97 (1)
c, Å	21.181 (9)	21.673 (6)	19.762 (5)
α, deg	75.50 (4)	90.00	90.00
β, deg	74.74 (3)	105.15 (3)	130.49 (1)
γ, deg	81.40 (4)	90.00	90.00
Z; V, Å^3	2; 2250 (2)	2; 3299 (2)	4; 4680 (5)
space group	$P\bar{1}$ (No. 2)	$P2_1/n$ (No. 14)	$C2/c$ (No. 9)
D_{calc}, g/cm^3	2.17	1.88	2.19
μ(Mo Kα), cm^{-1}	106	73	110
cryst size, mm	0.05 × 0.08 × 0.21	0.07 × 0.10 × 0.31	0.10 × 0.13 × 0.31
min, max abs cor	0.78, 0.98	0.73, 1.46	0.67, 1.17
$R(F)$, %	5.5	6.2	7.6
$R_w(F)$, %	6.8	6.5	7.9

studies on metal polysulfides in the last decade.[3,4] We have been interested in the chemistry of late-transition-metal polyselenides, including the group 11 metals because their corresponding polysulfides represent one of the most structurally wealthy triads in the periodic table.[3] Recently, we reported on the chemistry of silver–polyselenide complexes, a system characterized by great structural diversity.[5-7] Furthermore, our preliminary exploration on the Au/Se_x^{2-} system revealed an intriguing and unanticipated redox chemistry.[8] The reaction of $AuCl_3$ with Na_2Se_5 resulted in the isolation of $[Se(Se_5)_2]^{2-}$, an oxidation product of Na_2Se_5, while replacement of AuCN for $AuCl_3$ in the presence of $[(Ph_3P)_2N]Cl$ gave $[Au_2Se_2(Se_4)_2]^{2-}$, a Au(III) compound. In the latter complex, Se_5^{2-} was reduced by Au(I) to shorter fragments. This interesting redox interplay between Au^{n+} (n = 1, 3) and Se_x^{2-} incited us to investigate further this system in order to gain more information and insight into the redox behavior of gold in the presence of Se_x^{2-} ligands. In order to influence the aforementioned redox chemistry, we examined the reactivity of AuCN toward less reducible shorter polyselenide Se_x^{2-} ligands (i.e. x = 1–4) in the presence of different counterions such as Ph_4P^+, $[(Ph_3P)_2N]^+$, Pr_4N^+, etc. Here we wish to report the newly isolated $(Ph_4P)_2[Au_2(Se_2)(Se_3)]$ (I), $[(Ph_3P)_2N]_2[Au_2(Se_2)(Se_3)]$ (II), and $(Ph_4P)_2[Au_2(Se_2)(Se_4)]$ (III), the first Au(I) polyselenide complexes isolated from solution.

Experimental Section

Chemicals in this work were used as obtained. Dimethylformamide (DMF) was distilled under vacuum after being stored over 4A Linde molecular sieves for several days. Diethyl ether was distilled with potassium metal in the presence of benzophenone and triethylene glycol–dimethyl ether under a nitrogen blanket. All syntheses were carried out in a glovebox (Vacuum Atmospheres, Inc.). Na_2Se_x (x = 2, 3) and K_2Se_4 were prepared by reacting stoichiometric amounts of alkali metal with elemental selenium in liquid NH_3.

Preparation of $(Ph_4P)_2[Au_2(Se_2)(Se_3)]$ (I). Method A. A 45-mg (0.2-mmol) sample of solid AuCN was added to a 30-mL DMF suspension of 120 mg (0.6 mmol) of Na_2Se_2 in the presence of 75 mg (0.2 mmol) of Ph_4PCl. Upon stirring, a red solution was gradually formed in about 1 h. Following filtration of any formed precipitates, 30 mL of ether was added to the filtrate. Red, needle-shaped X-ray-quality single crystals of $(Ph_4P)_2[Au_2(Se_2)(Se_3)]$ were afforded within 2 days in 56% yield.

Method B. The reaction of AuCN with Na_2Se_3 in the same molar ratio and under the same conditions also gave I in 58% yield.

Preparation of $[(Ph_3P)_2N]_2[Au_2(Se_2)(Se_3)]$ (II). The reaction of 45 mg (0.2 mmol) of solid AuCN with 113 mg (0.4 mmol) Na_2Se_3 and 230 mg (0.4 mmol) of $[(Ph_3P)_2N]Cl$ in 30 mL of DMF gave a red solution within 1 h. Filtration of the reaction solution, followed by slow diffusion of 15 mL of ether into the filtrate, resulted in red crystals of $[(Ph_3P)_2N]_2[Au_2(Se_2)(Se_3)]$ in 52% yield within 6 days.

Table II. Positional Parameters and B_{eq} Values for the $[Au_2(Se_2)(Se_3)]^{2-}$ Anion in I (Standard Deviations in Parentheses)

atom	x	y	z	B, Å^2
Au(1)	0.0120 (1)	0.1525 (1)	0.24575 (5)	2.30 (2)
Au(2)	−0.0779 (1)	−0.1051 (1)	0.26774 (6)	3.12 (3)
Se(1)	0.0152 (3)	0.0836 (3)	0.3616 (1)	3.42 (7)
Se(2)	−0.0650 (3)	−0.1194 (3)	0.3808 (2)	3.66 (8)
Se(3)	−0.1041 (3)	−0.0872 (3)	0.1564 (2)	4.52 (7)
Se(4)	0.0583 (4)	0.0419 (4)	0.0940 (2)	5.9 (1)
Se(5)	0.0003 (3)	0.2251 (3)	0.1304 (1)	3.51 (7)

Table III. Positional Parameters and B_{eq} Values for the $[Au_2(Se_2)(Se_4)]^{2-}$ Anion in III (Standard Deviations in Parentheses)

atom	x	y	z	B(eq), Å^2
Au	0.93180 (6)	0.1557 (2)	0.6595 (1)	5.23 (7)
Se(1)	0.9571 (2)	0.3702 (4)	0.6689 (3)	8.5 (3)
Se(2)	0.8893 (2)	−0.0390 (4)	0.6387 (2)	5.4 (2)
Se(3)	0.9635 (2)	−0.1731 (4)	0.6735 (2)	5.3 (2)

Preparation of $(Ph_4P)_2[Au_2(Se_2)(Se_4)]$ (III). The procedure was identical with the one described above in method A except 140 mg (0.4 mmol) of K_2Se_4 was used. Analytically pure red needles were isolated in 76% yield.

IR Spectroscopy. FT-IR spectra of the solid compounds were determined in a CsI matrix. Each sample was ground with dry CsI into a fine powder, which was pressed to a transluscent pellet. The spectra were recorded in the far-IR region (500–100 cm^{-1}) with the use of a Nicolet 740 FT-IR spectrometer.

X-ray Diffraction and Crystallographic Studies. All compounds were scrutinized by the Debye-Scherrer X-ray powder diffraction method for the purpose of phase identification. Each sample was ground into a fine powder and packed into a 0.5-mm glass capillary, which was then sealed and mounted on a standard Debye–Scherrer powder camera. The XRD patterns were recorded photographically by using the Ni-filtered Cu radiation obtained from a Phillips Norelco XRG-5000 X-ray generator. Accurate d spacings (Å) for each compound were obtained from the XRD patterns recorded on a Phillips XRG-3000 computer-controlled powder diffractometer. The experimentally measured X-ray powder diffraction patterns of I–III correspond to those calculated from the single-crystal X-ray data.[9]

The crystallographic data sets of II and III were collected on a Rigaku AFC6S four-circle diffractometer with ω–2θ scan techniques and Mo Kα radiation. The crystals were mounted in glass capillaries and sealed. A crystal of compound I was affixed to the tip of a glass fiber, and the intensity data were measured at −93 °C on a Nicolet P3 diffractometer with a θ–2θ scan mode and Mo Kα radiation. The stability of the experimental setup and crystal integrity for each data collection were monitored by measuring three representative reflections periodically (every 100 or 150). No crystal decay was ever detected. Empirical absorption corrections were applied to all data based on ψ scans of several

(2) (a) Ansari, M. A.; Ibers, J. A. *Coord. Chem. Rev.* **1990**, *100*, 223–266. (b) Kolis, J. W. *Coord. Chem. Rev.* **1990**, *105*, 195–219.
(3) Draganjac, M.; Rauchfuss, T. B. *Angew. Chem., Int. Ed. Engl.* **1985**, *24*, 742–757.
(4) Müller, A. *Polyhedron* **1986**, *5*, 323–340.
(5) Kanatzidis, M. G.; Huang, S.-P. *J. Am. Chem. Soc.* **1989**, *111*, 760–761.
(6) Kanatzidis, M. G.; Huang, S.-P. *Angew. Chem., Int. Ed. Engl.* **1989**, *28*, 1513–1514.
(7) Huang, S.-P.; Kanatzidis, M. G. *Inorg. Chem.* **1991**, *30*, 1455–1466.
(8) Kanatzidis, M. G.; Huang, S.-P. *Inorg. Chem.* **1989**, *28*, 4667–4669.
(9) Smith, D. K.; Nichols, M. C.; Zolensky, M. E. POWD10: A Fortran IV Program for Calculating X-ray Powder Diffraction Patterns, Version 10. Pennsylvania State University, 1983.

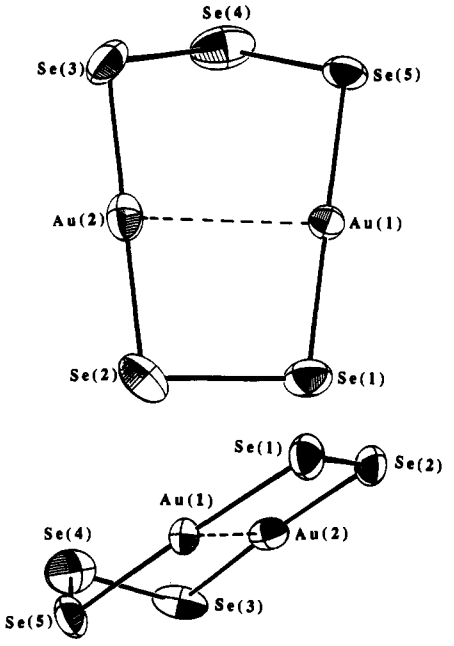

Figure 1. ORTEP representations of the $[Au_2(Se_2)(Se_3)]^{2-}$ anion in I with labeling scheme (two views). Selected distances (Å) and angles (deg): Au(1)–Se(1) = 2.388 (3), Au(1)–Se(5) = 2.401 (3), Au(2)–Se(2) = 2.399 (4), Au(2)–Se(3) = 2.401 (4), Se(1)–Se(2) = 2.402 (5), Se(3)–Se(4) = 2.283 (5), Se(4)–Se(5) = 2.279 (6), Au(1)–Au(2) = 3.004 (2); Se(1)–Au(1)–Se(5) = 177.9 (1), Se(2)–Au(2)–Se(3) = 176.8 (1), Au(1)–Se(1)–Se(2) = 97.7 (2), Au(2)–Se(2)–Se(1) = 96.8 (1), Au(1)–Se(5)–Se(4) = 100.8 (1), Au(2)–Se(3)–Se(4) = 101.3 (2), Se(3)–Se(4)–Se(5) = 105.2 (2).

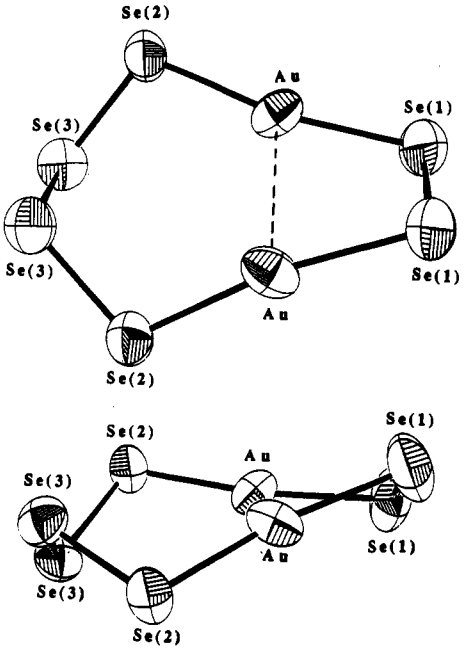

Figure 2. ORTEP representations of the $[Au_2(Se_2)(Se_4)]^{2-}$ anion in III with labeling scheme (two views). Selected distances (Å) and angles (deg): Au–Se(1) = 2.433 (5), Au–Se(2) = 2.355 (5), Se(1)–Se(1) = 2.46 (1), Se(2)–Se(2) = 2.280 (6), Se(3)–Se(3) = 2.301 (7), Au–Au = 3.132 (3); Se(1)–Au–Se(2) = 169.6 (1), Au–Se(1)–Se(1) = 95.4 (1), Au–Se(2)–Se(3) = 105.3 (2), Se(2)–Se(3)–Se(3) = 105.3 (2).

strong reflections with $\chi \sim 90°$. The structures were solved with direct methods and refined with full-matrix least-squares techniques. The calculations were performed on a VAXstation 2000 computer using the TEXSAN crystallographic software package of the Molecular Structure Corp. or the SHELXS-86 and SDP combined package of crystallographic programs.[10] The structure of II was found to be disordered at the anion site. The seven-membered ring of $[Au_2(Se_2)(Se_3)]^{2-}$ is positioned on a inversion center, causing the molecule to stack in two opposite directions in the crystal lattice. The two molecular orientations share a common Au–Au axis. The inversion center is situated in the middle of the Au–Au distance. The structure refinement for this compound was carried out on a disordered model with five Se atoms being of half-occupancy. No accurate structural parameters were obtainable due to the closeness of the disordered Se atoms. Nevertheless, all the bond distances and angles in this structure are comparable to those of the anion in the $(Ph_4P)_2[Au_2(Se_2)(Se_3)]$. The $2\theta_{max}$ values for I–III were 45, 40, and 45°, respectively. Table I gives crystal data and details for structure analysis of all compounds. All non-hydrogen atoms were refined either isotropically or anisotropically. The hydrogen positions were calculated but not refined. The final coordinates and average temperature factors of the atoms in the anions of I and III are given in Tables II and III.

Results and Discussion

Compounds I and II contain the same anion, $[Au_2(Se_2)(Se_3)]^{2-}$, which forms an envelope-shaped seven-membered ring containing two gold and five selenium atoms. The refined structure of the anion in $(Ph_4P)_2[Au_2(Se_2)(Se_3)]$ is shown in Figure 1. It has a C_s symmetry and features two linearly coordinated Au(I) centers bridged by Se_2^{2-} and Se_3^{2-} ligands. Two Au^+ ions and their adjacent Se atoms (e.g. Au(1)/Se(1)/Se(2)/Au(2)/Se(3)/Se(5)) form almost a perfect plane with the Se(4) atom being 1.172 Å above it. The Au–Se bonds are similar and average at 2.397 (5) Å. The Au···Au distance is 3.004 (2) Å, comparable with the other reported Au···Au distances in Au^+/polychalcogenide compounds.[11-14] The Se(1)–Se(2) distance in the diselenide unit is rather long at 2.402 (5) Å. The Se–Se bonds in the Se_3^{2-} unit, Se(3)–Se(4) of 2.283 (5) Å and Se(4)–Se(5) of 2.280 (9) Å, are in the normal range of Se–Se bond distances. Other selected metric parameters are given in the caption in Figure 1.

The $[Au_2(Se_2)(Se_4)]^{2-}$ anion in III is structurally similar to $[Au_2(Se_2)(Se_3)]^{2-}$, as shown in Figure 2. It has a C_2 symmetry with the 2-fold axis running across the centers of the Au···Au and Se(1)–Se(1) axes. The Au–Au separation between the two linearly coordinated Au atoms is 3.132 (3) Å (vs 3.004 Å in I) perhaps due to the longer Se_4^{2-} ligand present in the structure. Interestingly, the Au–Se bond lengths separate into two sets. The Au–Se bonds to Se_2^{2-} are long at 2.433 (5) Å, while the Au–Se bonds to Se_4^{2-} are short at 2.355 (5) Å. By comparison, the average Au–Se distance in the polymeric $[Au(Se_5)]_n^{n-}$[15] is 2.410 (4) Å. Although the Se–Se bond distances in Se_4^{2-} are all normal, the Se–Se distance of 2.46 (1) Å in Se_2^{2-} is even longer than that in I. The eight-membered ring is puckered. Other selected metric parameters are given in the caption of Figure 2.

The long Se(1)–Se(2) distance of the Se_2^{2-} unit in both compounds suggests considerable strain and probably originates from the need of this unit to span the Au···Au distance. Instead of forming a molecule with Se_2^{2-} ligands on both sides, I adopts a Se_3^{2-} ligand on one side and a Se_2^{2-} on the other. The Se–Se bond in Se_2^{2-} cannot be stretched to such a distance as to accommodate two Au atoms 2.9–3.0 Å apart, to form a planar molecule of $[Au_2(Se_2)_2]^{2-}$. This would cause severe deviations in the linear coordination of Au. This structure is only found possible in the

(10) (a) TEXSAN: Single Crystal Structure Analysis Software, Version 5.0. Molecular Structure Corp., The Woodlands, TX. (b) Sheldrick, G. M. In *Crystallographic Computing 3*; Sheldrick, G. M., Kruger, C., Doddard, R. Oxford University Press: Oxford, U.K., 1985; pp 175–189. (c) Frenz, B. A. The Enraf-Nonius CAD4 SDP System. In *Computing in Crystallography*; Delft University Press: Delft, Holland, 1978; pp 64–71.

(11) Müller, A.; Römer, M.; Bögge, H.; Krickemeyer, E.; Schmitz, K. *Inorg. Chim. Acta* **1984**, *B5*, L39–L41.

(12) Marbach, G.; Strähle, J. *Angew. Chem., Int. Ed. Engl.* **1984**, *23*, 715–716.

(13) Haushalter, R. C. *Inorg. Chim. Acta* **1985**, *102*, L37–L38.

(14) (a) Adel, J.; Weller, F.; Dehnicke, K. *Z. Naturforsch.* **1988**, *43B*, 1094–1100. (b) Kanatzidis, M. G. *Abstracts of Papers*, 196th National Meeting of the American Chemical Society, Los Angeles, CA; American Chemical Society: Washington, DC, 1988; INORG 469. (c) Banda, R. M. H.; Cusick, J.; Scudder, M. L.; Craig, D. C.; Dance, I. G. *Polyhedron* **1989**, *8*, 1995–1998. (d) Kanatzidis, M. G.; Dhingra, S. *Inorg. Chem.* **1989**, *28*, 2024–2026.

(15) Park, Y.; Kanatzidis, M. G. *Angew. Chem., Int. Ed. Engl.* **1990**, *29*, 914–915.

Scheme I

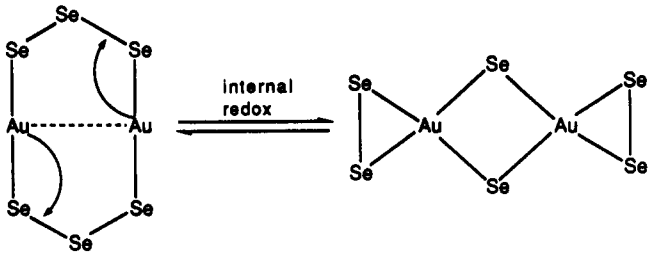

Au^+/Te_2^{2-} system (i.e. $[Au_2(Te_2)_2]^{2-}$),[13] where the Te–Te distance is 2.781 Å, closer to the Au–Au distance of 2.908 Å. In anticipation that a symmetrical molecule such as $[Au_2(Se_3)_2]^{2-}$ or $[Au_2(Se_4)_2]^{2-}$ might form with higher concentration of longer polyselenides in solution, we used Se_4^{2-} instead of the original Se_2^{2-} and Se_3^{2-}. Unexpectedly, the isolated molecule, III, contains a Se_2^{2-} unit bridging the two gold atoms while a Se_4^{2-} ligand is adopted on the other side. The fact that the more symmetric compound $(Ph_4P)_2[Au_2(Se_x)_2]$ (x = 3, 4) does not form is intriguing, in view of the apparent stability of a sulfur analogue, $[Au_2(S_4)_2]^{2-}$.[11] The reason for the preferential formation of I–III might rest with the stability of the $Au_2(Se_2)$ unit. It might be reasonably speculated that if indeed $[Au^I_2(Se_x)_2]^{2-}$ (x = 3, 4) formed in solution, it could be susceptible to internal redox electron transfer between Au(I) and Se–Se bonds according to Scheme I. This is similar to that thought to occur in the formation of $[(Ph_3P)_2N]_2[Au^{III}_2Se_2(Se_4)_2]$.[8] However, it is more difficult to reduce the Se–Se bonds in Se_2^{2-} than those in Se_3^{2-} or Se_4^{2-}. The species $[Au^{III}_2Se_2(Se_x)_2]^{2-}$ (x = 2, 3) formed by the internal electron transfer may not be favored under such conditions due to the small size of the Se_x^{2-} ligand, which cannot span the square-planar gold coordination site. The work presented here suggests that the Au(I) vs Au(III) interplay is largely dominated by the size of the Se_x^{2-} ligands. This is an exception to the widely accepted view that ligand preferences of the metal ions are more important in determining structure than the sizes of the Se_x^{2-} ligands used. This is certainly true with divalent and trivalent ions such as Cd^{2+}, Ni^{2+}, and In^{3+}.[14]

At this point, it is relevant to discuss the polymeric polyselenide $KAuSe_5$.[15] The structure consists of dimeric one-dimensional $[AuSe_5]_n^{n-}$ anionic chains with linearly coordinated Au(I) atoms being bridged by long open chains of Se_5^{2-} ligands.[8] The Au(I)–Au(I) distance between two chains is 2.95 Å. It is interesting that oxidation of this compound to a Au(III) species does not occur despite the existence of Se_5^{2-} ligands. However, the compound was prepared in molten Se_x^{2-}, in which different equilibria might be operable, and it was found that indeed slight deviations from the optimum Au/Se_x^{2-} ratio *do* induce redox chemistry and formation of Au(III) compounds.[15]

Compounds I and II have identical far-IR spectra showing absorptions at 265 and 236 cm^{-1}. The spectrum of compound III is similar, but an additional peak appears at 257 cm^{-1}. The strongest peak in all spectra is at 236 cm^{-1}. The absorptions at 265 and 257 cm^{-1} can be attributed to Se–Se stretching vibrations,[7] while those at 236 cm^{-1} most likely arise from Au–Se stretching vibrations.

The isolation of two Au(I) polyselenide compounds in this work and the Au(III) species in the previous report[8] as a function of Se_x^{2-} length and counterion size attests to the vacillating nature of redox chemistry between Au(I)/Au(III) and polyselenide ligands and suggests that considerably more chemistry would be possible in this system. Analogous redox chemistry with corresponding S_x^{2-} and Te_x^{2-} ligands remains to be seen.[16]

Acknowledgment. Financial support from the donors of the Petroleum Research Fund, administered by the American Chemical Society, is gratefully acknowledged. We are grateful to the National Science Foundation for a Presidential Young Investigator Award.

(16) Huang, S.-P.; Kanatzidis, M. G. Work in progress.

Supplementary Material Available: Tables of crystal structure analyses, atomic coordinates of all atoms, and anisotropic and isotropic thermal parameters of all non-hydrogen atoms, and calculated and observed powder patterns for I–III (24 pages); listings of calculated and observed ($10F_o/10F_c$) structure factors for I–III (54 pages). Ordering information is given on any current masthead page.

Contribution from the Department of Chemistry,
Faculty of Engineering Science,
Osaka University, Toyonaka, Osaka 560, Japan

Mixed-Metal Chloro Sulfido Cluster Complex of Molybdenum and Platinum, $[Mo_3Pt_2S_4Cl_4(PEt_3)_6]$

Taro Saito,*,† Toshio Tsuboi, Yoshimichi Kajitani,
Tsuneaki Yamagata, and Hideo Imoto†

Received January 30, 1991

In our recent publication, syntheses of mixed-metal chloro sulfido and chloro selenido complexes of molybdenum and nickel were reported.[1] They were prepared by the reaction of $[Mo_3X_4Cl_4(PEt_3)_3(MeOH)_2]$ (X = S, Se)[2] with $Ni(cod)_2$ (cod = 1,5-cyclooctadiene). In the present study, another excellent building block compound, $Pt(cod)_2$,[3] was reacted with the same trinuclear molybdenum complex, and the mixed-metal cluster complex $[Mo_3Pt_2S_4Cl_4(PEt_3)_6]$ (**1**) with an unexpected structure was obtained.

Experimental Section

Synthesis. A solution of $Pt(cod)_2$[4] (0.18 g, 0.44 mmol) in THF (20 mL) was mixed with a toluene solution of triethylphosphine (0.4 mL, 0.66 mmol) and stirred for 30 min. To the resulting deep yellow solution was added $[Mo_3S_4Cl_4(PEt_3)_3(MeOH)_2]$ (0.23 g, 0.22 mmol). The solution was stirred at room temperature, and its color gradually changed to green. After 8 h, the solvent, triethylphosphine, and cyclooctadiene were removed under reduced pressure, and the residue was washed with hexane (2 × 7 mL). The soluble component was extracted with ether (3 × 40 mL), and removal of ether formed a green powder. Recrystallization of the solid from THF–hexane gave dark green needles (0.18 g). Anal. Calcd for $C_{38}H_{94}Cl_4Mo_3O_{0.5}P_6Pt_2S_4$: C, 26.96; H, 5.60; Cl, 8.38; Mo, 17.00; Pt, 23.04. Found: C, 27.06; H, 5.40; Cl, 8.32; Mo, 17.5; Pt, 23.4. ^{195}Pt NMR (in 25% toluene-d_8; 106.95 MHz; Na_2PtCl_6 as an external reference): δ −4560 (dd with satellites due to a Pt–Pt coupling of 700 Hz;[5] J_{Pt-P} = 4410, 3100 Hz). The complex is air-sensitive and decomposed gradually in the crystalline state and rapidly in solution when exposed to air.

X-ray Structure Determination. Single crystals of **1** were sealed in glass capillary tubes under dinitrogen for the X-ray measurements. The intensity data were collected by a Rigaku AFC-5 diffractometer equipped with a Rotaflex rotating anode X-ray generator. The data showed the structure had the *C*-centered orthorhombic symmetry, and the observed systematic absences indicated the space group *Cmca* or *C2ca*. The structure could be solved only by *C2ca*, and the setting of the cell was transformed so that the structure had the standard symmetry *Aba2*. The positions of metal atoms were determined by direct methods (MULTAN78), and other non-hydrogen atoms were located on the Fourier maps. Though it was not possible to distinguish chlorine and sulfur atoms from the X-ray data, we assigned all bridging ligand atoms to sulfur for the following reasons. (1) The observed bond distances of terminal ligands with molybdenum atoms are longer than those of the bridging ligands, and the Mo–S distances are generally shorter than the Mo–Cl distances. (2) Terminal sulfido ligands are rare while terminal chlorine atoms are common. (3) It is unlikely that the central part $[Mo_3S_4]$ of the starting complex rearranges during the preparation reaction. The THF molecule was found on the 2-fold axis as broad Fourier peaks, and it was treated as a rigid C_5 pentagon with a C–C distance of 1.52 Å. All carbon atoms were treated isotropically while all other non-hydrogen atoms were treated anisotropically. In the final full-matrix least-squares refinements, hydrogen atoms were included at calculated positions (C–H = 0.92 Å) with a fixed thermal parameter. If the enantiomeric structure was as-

† Present address: The Department of Chemistry, Faculty of Science, The University of Tokyo, Hongo, Tokyo, 113, Japan.

0020-1669/91/1330-3575$02.50/0